Magneto-Optical Detection of Synthetic Malaria Pigment in Photonic Crystal Fiber

Saeed Azad, Ahmad Al-Shboul, Christian Lacroix, Ricardo Izquierdo, David Ménard, Martin Olivier, Carlos Villalba Guerrero, Bora Ung

***Abstract*— The necessity to develop new technologies for high-sensitivity malaria diagnosis has sparked a global effort in medical and integrative sciences. Most developing procedures rely on research-grade instruments, sophisticated assays, or on expertise. In this work, we propose an alternative optical methodology using a compact and user-friendly apparatus based on a photonic crystal fiber (PCF). Malaria pigment known as hemozoin is an insoluble reddish brown microcrystalline. These crystallites stand out from other blood components in terms of their exceptional magneto-optical features. Consequently, they can function as spinning entities in suspension in response to the external magnetic field. Here synthetic hemozoin (SHz) was obtained in a forthright way with a high yield of 75%. In addition, the prepared sample was characterized morphologically and structurally. The PCF's nanoholes were filled with the aqueous suspension of SHz with various concentrations and transmitted power recorded in response to the magnetic field. We demonstrate a sensor with a detection threshold of 7.2 parasite/*μ*l well below the level of clinical relevance (50-100 parasite/*μ*l) at a very small liquid sample (less than 0.5 *μ*l). The results of this investigation may provide new light on potential medicinal and sensor applications.**

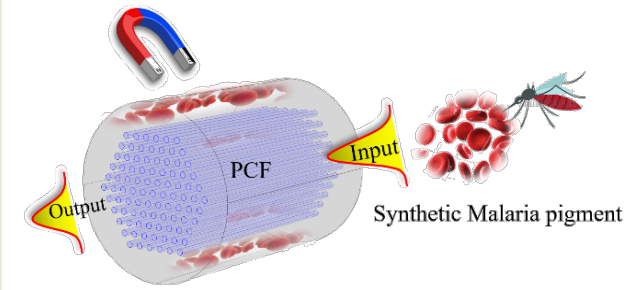

***Index Terms*— Malaria pigment, Magneto-optical detection of Malaria, Photonic Crystal Fiber,**

I. Introduction

Plasmodium falciparum (P. falciparum) causes the greatest and the harshest form of Malaria among the five protozoan species with 90% of total deaths. It is an infection that strikes between 300 to 500 million people globally and causes 1.5 to 2.7 deaths annually[1]. It remains the most common vector-borne infectious disease despite global attempts to eradicate it, including preventive measures and pharmacological regimens. The global effort to eliminate malaria is severely hampered by the parasites' growing medication resistance, and climate change may potentially bring back malaria mosquitoes in areas that were previously free of them. The creation of inexpensive diagnostic techniques that are reliable even at an early stage of infection could lead to a major improvement. The most accurate and sensitive diagnostic technique currently in use is the microscopic examination of blood smears to evaluate parasitemia, which is defined as 20 parasites in 1 µl of blood[2]. This test is costly and time-consuming because it calls for special training and powerful microscopes. On the other hand, rapid diagnostic tests (RDT) that use antigen-based detection of malaria parasites are not only quick but also more affordable[3], [4]. However, the sensitivity threshold for RDTs is limited to around 100 parasites/µl; which is not sensitive enough to reliably detect the early-stages of infections. Although polymerase chain reaction (PCR) analysis is sensitive enough to detect even 1 parasite/µl among molecular biology-based techniques, the practical application of PCR analysis in the field is limited due to the requirements of advanced technology and expertise. Extensive study and a vast array of diagnostic schemes have been offered in the last few years because of the necessity to develop new diagnostic procedures. Some instances include selective microscopic detection of infected blood cells such as third harmonic

Bora ung (Corresponding author), Saeed Azad, Ahmad Al-Shboul, and Ricardo Izquierdo are with department of electrical engineering and LACIME, École de technologie supérieure university, Montreal H3C 1K3, Canada (e-mail: bora.ung@etsmtl.ca, saeedazad64@gmail.com, ahmad.al-shboul.1@ens.etsmtl.ca, ricardo.izquierdo@etsmtl.ca). E Christian Lacroix and David Ménard are with department of engineering physics, Regroupement Québécois sur les Matériaux de Pointe (RQMP), Polytechnique Montréal, Montréal, Canada H3T 1J4(e-mail : c.lacroix@polymtl.ca, david.menard@polymtl.ca). Martin Olivier and Carlos Villalba Guerrero are with the research institute of the McGill university health centre, Program in Infectious Diseases and Immunology in Global Health, Departments of Medicine, Microbiology and Immunology, McGill University, Montreal, Canada(e-mail; martin.olivier@mcgill.ca, carlos.villalbaguerrero@mail.mcgill.ca)

generation microscopy[5], magnetic deposition microscopy[6], photoacoustic spectroscopy[7]and cell microarray chips[8]. On the other hand, a growing number of approaches use malaria pigments as the target molecules based on their magnetic properties, including magneto-optical detection with polarized light[9], [10] enhanced resonance Raman spectroscopy using magnetic field enriched surface[11], magneto immunoassays[12] as well as intensity based malaria screening[13]. Malaria pigment known as hemozoin is a byproduct of the disease formed during the intraerythrocytic growth cycle of the parasites. Malaria parasites digest the hemoglobin of blood which leads to the accumulation of monomeric heme. Since it is highly toxic to the parasites, they transform heme into an insoluble crystallized form[14]. During this process, low-spin diamagnetic Fe^{2+} ions change into high spin (S=5/2) paramagnetic Fe^{3+} ions in hemozoin. Hemozoin has a triclinic crystal structure with various morphologies depending on the parasite species[15]. They usually have an elongated rod-like shape with a length ranging from 300 nm to 1 µm. Natural hemozoin (nHz) preparation is a time-consuming process that requires competence to infect the living being and extract the product. As a result, researchers prefer to deal with synthetic hemozoin (SHz) or β-hematin, different methods have been established for its artificial synthesis [16], [17]. The synthetic grown version exhibited a similar crystal structure[18], optical and magnetic properties to natural hemozoin[19], [20]. There are various publications that address the synthesis of SHz and its physicochemical properties[18],[21]–[23], to the best of our knowledge no study has produced SHz of comparable size to natural ones as well as measuring the refractive index (RI) of aqueous solution of SHz and assessed the susceptibility of that all in one study.

The technical novelty of this work is related to the application of PCF in conjunction with microcrystal of SHz. Previously, some papers proposed the application of infiltrated PCF with ferrofluids for magnetic field sensing applications [24], [25].

In this work, we present a novel method for the rapid monitoring of synthetic malaria pigment crystals. which in contrast to the majority of the previously described emerging approaches, it might be realized as a compact diagnostic tool. In addition, the controlled procedure that enables to produce SHz samples with similar dimensions to the naturally occurring Hz provided through a straightforward process. Finally, The detection threshold of our instrument for the aqueous solution of SHz is 0.8pM to a level of parasitemia 7.2 parasite/µl that is below clinical relevance(<50-100 parasite/µl)[9], [26]. Clinical trials will be required to prove this, but the detection limit achieved is already a significant improvement over RDTs.

II. Materials And Methods

A. Materials

Hemin crystalline powder known as Chloro(protoporphyrinato)iron (III), was purchased from Sigma-Aldrich. Other chemicals including sodium hydroxide (NaOH), methanol (CH_3OH), propionic acid ($C_3H_6O_2$), phosphorus pentoxide (P_2O_5), and bicarbonate sodium ($NaHCO_3$) were obtained from Thermo Fisher Scientific Chemicals, Inc. The PCF was manufactured in Laval university.

B. Mimic of Hemozoin: Synthesis Process

Synthetic hemozoin (SHz) was obtained by dissolving NaOH powder (0.4 gr) in deionized (DI) water (100 ml). The aqueous solution was degassed with nitrogen (N_2) for 30 min. In the next step, 500 mg of hemin was added slowly and stirred gently at room temperature for 20 min. Then propionic acid was added via micropipette drop wisely with mild stirring for 40 min. The solution acidity was adjusted by propionic acid and monitored by a pH meter (Fisherbrand accumet) during adding acid. Initially the pH was 12.44 which was reduced to 3.3 with the acid addition. The well-stirred suspension was heated in an oil bath at 70°C for 17h to provide uniform and stable reaction conditions. The achieved mixture was cooled at room temperature and decantated via micropipette. To purify the product, it was washed extensively with $NaHCO_3$ (0.1M), methanol, and water three times. The SHz product was finally dried in the oven at 40°C for 48h over P_2O_5. The applied technique yielded more than 75 percent of the product.

III. Characterization of SHz

A. Fourier-Transform Infrared (FTIR) Spectroscopy

To investigate the chemical structure of SHz, FTIR spectroscopy was employed. To acquire IR spectra small portion of SHz powder was positioned on the diamond crystal of the spectrometer (model: Nicolet 6700 /Smart ITR, Thermo Scientific) and compressed. The spectra were recorded in reflection/ transmission mode over the range of wavenumber 2000-650 cm^{-1}, at the resolution of 2 cm^{-1} with 128 coadded scans. As shown in Fig. 1 SHz spectra exhibited specific sharp bands at 1660 cm^{-1} and 1209 cm^{-1} which were assigned to coordinated carbonyl (C=O) stretching vibrations and carboxylate (C—O) respectively[27], [28].

B. X-ray Powder Diffraction (XRD)

The D8 advance Bruker AXS diffractometer was used to acquire the XRD patterns of SHz's, using a copper-based radiation source (Cu K, 1.5406) over a range of 2θ= 5-30°. Fig. 1 displays the SHz's XRD pattern. The presence of sharp Bragg diffraction peaks, confirms a high crystallinity structure. The SHZ's unit cells are made up of two heme molecules each with symmetry-related interactions in a triclinic lattice structure[29]. The obtained sample exhibited different growth directions with priority at 2θ = 7° which corresponds to the (100)

plane.

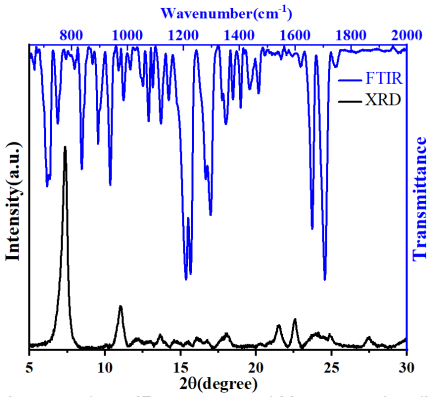

Fig. 1. Fourier-transform IR spectra and X-ray powder diffraction pattern of SHz

C. High-Resolution Scanning Electron Microscopy (HRSEM)

The morphology of SHz was investigated using HRSEM. Basically, most SHz possess higher dimensions compared to natural hemozoin. Here SHz samples prepared at lower pH (3.3) resulted in samples with dimensions comparable to their natural counterpart. As Shown in Fig. 2 (a) needle-like microcrystals with lengths less than one micron appeared. To assess the average size and uniformity of the obtained samples more than a hundred crystals were chosen from SEM images, and dimensions were analyzed using the Image J software. As shown in Fig. 2(b) the length of microcrystals mostly distributed between 400nm to 600nm with average length and diameter of 489 nm and 130 nm respectively.

D. Vibrating Sample Magnetometry (VSM)

The magnetization hysteresis loop was measured using a EV9 VSM from ADE Technologies. The obtained powders were weighted and exposed to an increasing magnetic field (up to 2 T) Then the field lowered to zero and increased again in opposite direction. In order to calculate the magnetization, the value of 1.44 g/cm^3 was considered as the density of hemozoin[30]. As shown in Fig. 3 the M-H curve presents the recorded values. The positive susceptibility of 1.4E-5 confirms the paramagnetic feature of SHz which arises from the presence of unpaired electrons in Fe^{3+} ions.

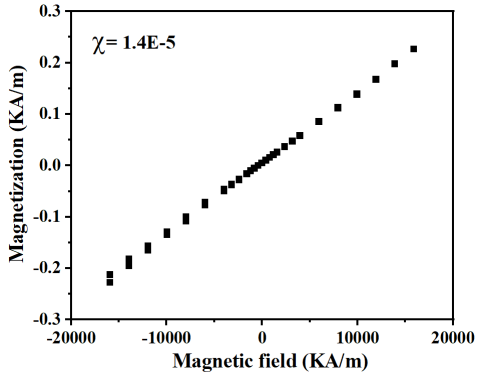

Fig. 3. M-H curve related to SHz.

E. Refractive Index (RI) Measurement

In order to model the transmitted light in the infiltrated photonic crystal fiber (PCF), it is crucial to define the proper RI that corresponds to different concentrations of SHz. In this regard, several aqueous solutions of SHz with different concentrations were prepared and poured into the quartz cuvette. When the He-Ne laser beam is incident at a small angle on the facet of the cuvette and passes through the cell, the propagation axis of the transmitted beam becomes displaced through refraction. The displacement (Δ) allows us to calculate the liquid's RI based on equation 1[31], [32].

$$n_1 = n_0 \sin\theta \sqrt{1 + \left[\frac{\cos\theta}{\sin\theta - \frac{\Delta}{d}}\right]^2} \quad (1)$$

Where n_1 stands for the RI of liquid, n_0 is the RI of the surrounding environment (air), θ the angle of incidence between the laser beam and the facet of the cuvette, while d=10 mm represents the internal length of the cuvette. The measured refractive index values as a function of the concentration of SHz samples are plotted in Fig. 4.

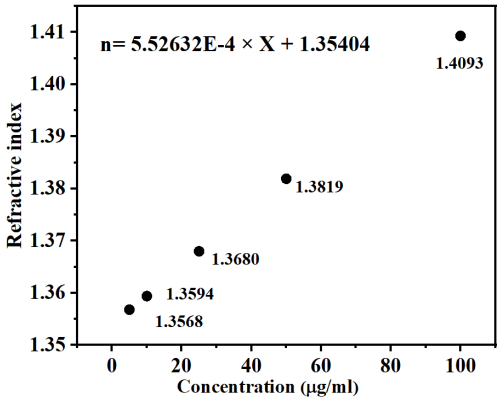

Fig. 4. Calculated refractive index of the aqueous solution of SHz with different concentration.

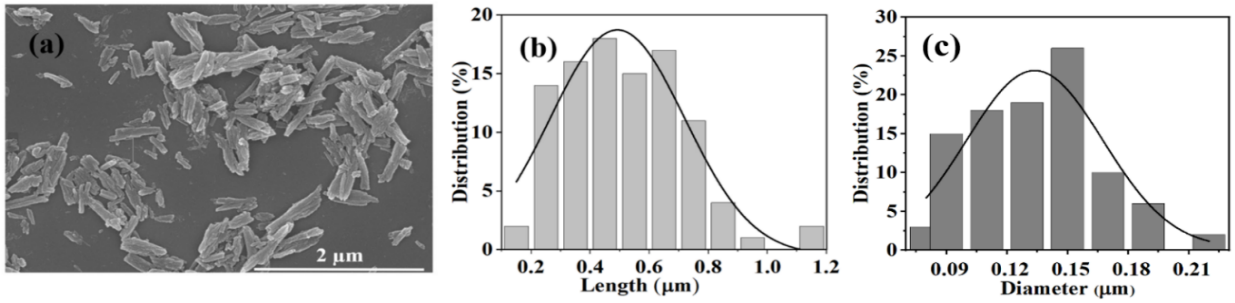

Fig. 2. (a) High-resolution scanning electron microscopy image of SHz, distribution histogram of synthetic hemozoin (b) length, (c) diameter.

IV. Detection Principle

Basically as linearly polarized light passes through a disordered optical medium that subject to the external magnetic field, It can be affected by deflection, rotation in polarization and scattering that finally results in changes in refractive indices[24], [33], [34]. Hemozoin microcrystals possess a magnetic signature as well as an opaque intrinsic feature that offers key parameters for fabricating magneto-optical based sensors. Their paramagnetism is caused by the presence of high spin unpaired electrons in Fe^{3+} ions. When such crystallites are suspended in a liquid as shown in Fig. 5(e) upon exertion of an external magnetic field, they start to form chain like clusters and co-align along the direction of the magnetic field to gain magnetic energy[35] under this phenomenon the refractive index of liquid would change. By these changes in RI the transverse E-field distribution at the output facet of the fiber will be changed which corresponds to the leakage of guided light as shown in the CCD image of Fig. 5 (d).

Similar to this concept is well explained and modeled in our previous research [25]. Here, we propose a PCF infiltrated with an aqueous solution of SHz that provides a miniature sensor with the ability to guide most portion of light in the silica core which can detect small fraction of Hz

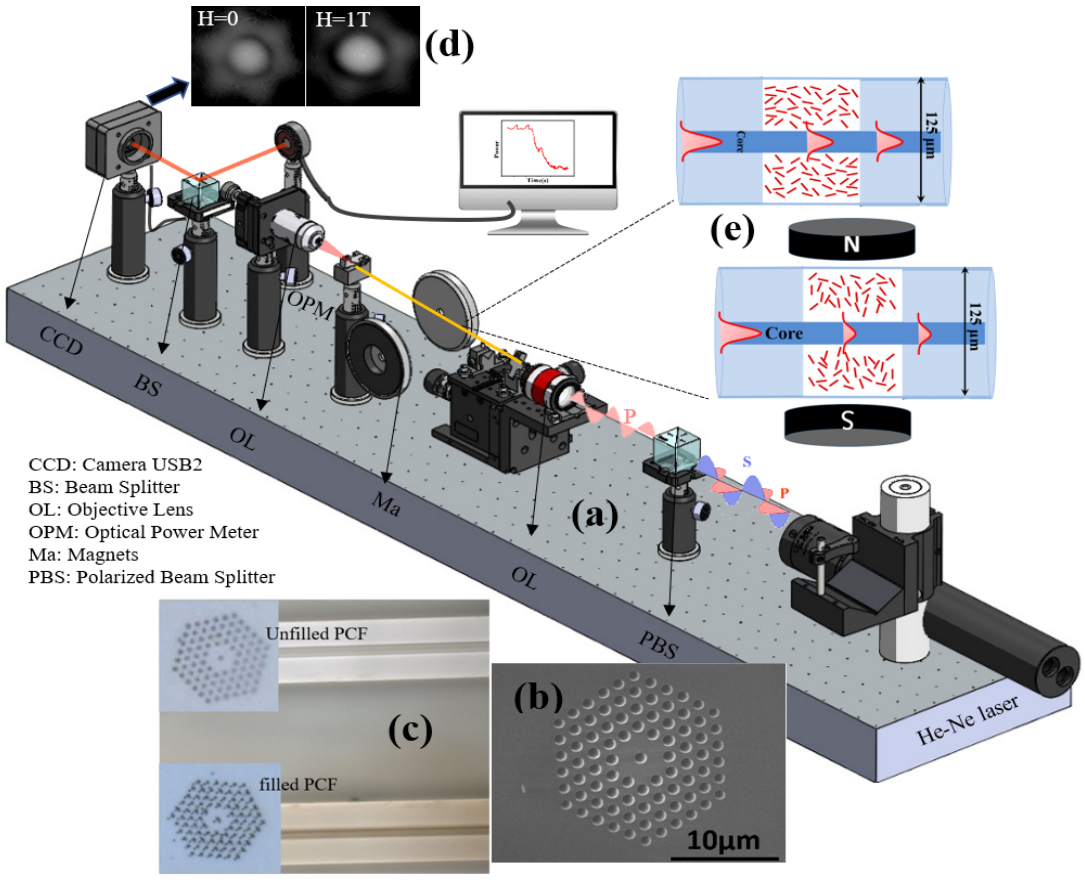

Fig. 5. (a) Schematic illustration of the experimental setup, (b) SEM cross section image of PCF (c) optical cross section and side image of unfilled and filled PCF(d) CCD image of output beam profile in H=0 and H≠0, (e) Distribution of Hz micro crystals in absence and presence of magnetic field.

in solution. Fig. 5(a) shows a schematic of the diagnostic setup, He-Ne laser source was chosen because light

absorption is weaker for water in the visible band compared to the near-infrared band. When the E-field of the guided light is parallel to the direction of the external magnetic field, optical absorption increases in fluids containing magnetic particles[36]. In practice, using a polarized beam splitter not only improves the interaction of light with SHz, but also reduces the fluctuation in output power and offers a higher signal-to-noise ratio. In the next step the collimated laser beam is coupled to the infiltrated fiber via a 20x objective lens. To fill micro holes of PCF we exploited Poiseuille law[37]. In this method, one end of the fiber is submerged in the solution and kept under high pressure (3 bar), while the other end is exposed to ambient pressure. The pressure difference enables the PCF to be filled with the liquid sample. Fig. 5(c) exhibits the optical microscopy images of the cross section and side view of the unfilled and filled fiber. As clearly observable the injected liquid came out of the tiny air holes when we did the cleave. The PCF contains holes with an average diameter of 1.2 μm and spaced with a period of 1.6 μm. The middle section of fiber with the length of 20 cm placed between two magnetic discs made of NdFeB that provided a uniform magnetic field of 1 T. To monitor the changes in output power and beam pattern at the same time during exertion of the magnetic field, the guided light on the other end of the fiber collimated and divided via 20x objective lens and beam splitter respectively. Fig. 6(a) presents the output power changes related to the PCF infiltrated with different concentrations of SHz upon application of the external magnetic field (1T). As expected, changes in power correspond to the concentrations of SHz in suspension. Furthermore, a sample consisting of sole distilled water was used as the reference (shown with solid black line). We observe that the reference sample did not affect the transmitted power. The sample with the lowest percentage of SHz, 0.8 pM (which corresponds to 7.2 parasite/μl that is in agreement with the relevant clinical concentration[2]), exhibited detectable changes in power variation in presence of magnetic field to the background noise with a minimum signal-to-noise ratio of 4.5 dB. The slight fluctuation in power is ascribed to the magnetophoretic movement of SHz micro crystals and random particle-particle interactions. The experiments were repeated several times and the average value of power changes and corresponding error bar for each concentration is shown in Fig. 6(b). Measurements indicate that the response time, the time-period during which the variation in optical power changes from 90% to 10%. of total power changes, increased from 41s to 205 s for samples with 0.8 pM to 16 pM concentrations of SHz, respectively as shown in Fig. 6(b).

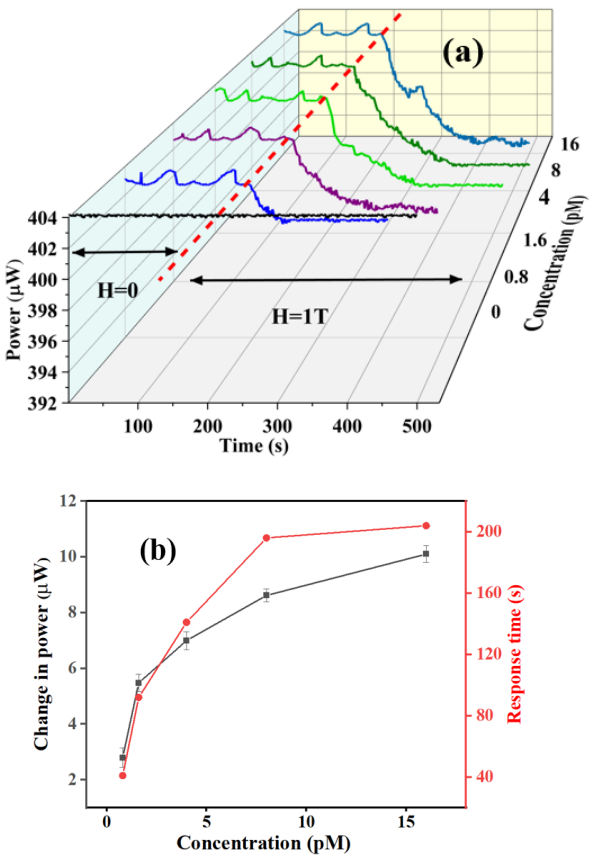

Fig. 6. (a) Response time of the proposed sensor in presence of external magnetic field (1T) and (b) Average changes in output power and response time for different concentrations of the SHz.

V. Conclusion

The fine precision of advanced optical fiber technologies in combination with functional fluids can offer a desirable diagnostic tool for emerging bio medical sensing applications. In this work, in the first step we synthesized the mimic of malaria pigment via straightforward technique with a yield reaches of 75 %. The RI of the SHz aqueous solution with different concentrations was measured which is rarely considered in literatures. In addition, the positive magnetic susceptibility of 1.4E-5 was determined from magnetometry measurements which confirms the paramagnetic behavior of SHz. We also demonstrate a novel magneto-optical malaria sensor using PCF with submicron air holes infiltrated by SHz suspension with the ability to detect SHz. The proposed configuration requires solely a tiny amount of liquid sample (0.5μl) for the detection of pigment crystals. The threshold detection limit was 7.2 parasite/μl with a full order of magnitude below the clinical level. A Simple magneto-optical configuration scheme and the ability to detect at point of care indicate a promising alternate technique for malaria detection compared to conventional methods.

REFERENCES

[1] M. Jaramillo *et al.*, "Synthetic Plasmodium-like hemozoin activates the immune response: a morphology-function study," *PloS one*, vol. 4, no. 9, p. e6957, 2009.

[2] K. V. Ragavan, S. Kumar, S. Swaraj, and S. Neethirajan, "Advances in biosensors and optical assays for diagnosis and detection of malaria," *Biosensors and Bioelectronics*, vol. 105, pp. 188–210, 2018.

[3] D. Bell, C. Wongsrichanalai, and J. W. Barnwell, "Ensuring quality and access for malaria diagnosis: how can it be achieved?," *Nature Reviews Microbiology*, vol. 4, no. 9, pp. S7–S20, 2006.

[4] M. L. Wilson, "Malaria rapid diagnostic tests," *Clinical infectious diseases*, vol. 54, no. 11, pp. 1637–1641, 2012.

[5] J. M. Bélisle *et al.*, "Sensitive detection of malaria infection by third harmonic generation imaging," *Biophysical journal*, vol. 94, no. 4, pp. L26–L28, 2008.

[6] P. A. Zimmerman, J. M. Thomson, H. Fujioka, W. E. Collins, and M. Zborowski, "Diagnosis of malaria by magnetic deposition microscopy," *The American journal of tropical medicine and hygiene*, vol. 74, no. 4, pp. 568–572, 2006.

[7] J. R. Custer, "Photoacoustic detection and spectral analysis of hemozoin in human leukocytes as an early indicator of malaria infection," PhD Thesis, University of Missouri–Columbia, 2011.

[8] S. Yatsushiro *et al.*, "Rapid and highly sensitive detection of malaria-infected erythrocytes using a cell microarray chip," *PLoS One*, vol. 5, no. 10, p. e13179, 2010.

[9] D. M. Newman *et al.*, "A magneto-optic route toward the in vivo diagnosis of malaria: preliminary results and preclinical trial data," *Biophysical journal*, vol. 95, no. 2, pp. 994–1000, 2008.

[10] P. F. Mens, R. J. Matelon, B. Y. M. Nour, D. M. Newman, and H. D. F. H. Schallig, "Laboratory evaluation on the sensitivity and specificity of a novel and rapid detection method for malaria diagnosis based on magneto-optical technology (MOT)," *Malaria journal*, vol. 9, no. 1, p. 207, 2010.

[11] C. Yuen and Q. Liu, "Magnetic field enriched surface enhanced resonance Raman spectroscopy for early malaria diagnosis," *Journal of biomedical optics*, vol. 17, no. 1, p. 017005, 2012.

[12] M. de Souza Castilho, T. Laube, H. Yamanaka, S. Alegret, and M. I. Pividori, "Magneto immunoassays for plasmodium falciparum histidine-rich protein 2 related to malaria based on magnetic nanoparticles," *Analytical chemistry*, vol. 83, no. 14, pp. 5570–5577, 2011.

[13] S. E. McBirney, D. Chen, A. Scholtz, H. Ameri, and A. M. Armani, "Rapid diagnostic for point-of-care malaria screening," *ACS sensors*, vol. 3, no. 7, pp. 1264–1270, 2018.

[14] A. F. Slater *et al.*, "An iron-carboxylate bond links the heme units of malaria pigment," *Proceedings of the National Academy of Sciences*, vol. 88, no. 2, pp. 325–329, 1991.

[15] M. F. Oliveira *et al.*, "Structural and morphological characterization of hemozoin produced by Schistosoma mansoni and Rhodnius prolixus," *Febs letters*, vol. 579, no. 27, pp. 6010–6016, 2005.

[16] I. Y. Gluzman, S. E. Francis, A. Oksman, C. E. Smith, K. L. Duffin, and D. E. Goldberg, "Order and specificity of the Plasmodium falciparum hemoglobin degradation pathway," *The Journal of clinical investigation*, vol. 93, no. 4, pp. 1602–1608, 1994.

[17] D. S. Bohle and J. B. Helms, "Synthesis of β-hematin by dehydrohalogenation of hemin," *Biochemical and biophysical research communications*, vol. 193, no. 2, pp. 504–508, 1993.

[18] S. Pagola, P. W. Stephens, D. S. Bohle, A. D. Kosar, and S. K. Madsen, "The structure of malaria pigment β-haematin," *Nature*, vol. 404, no. 6775, pp. 307–310, 2000.

[19] T. Frosch *et al.*, "In situ localization and structural analysis of the malaria pigment hemozoin," *The Journal of Physical Chemistry B*, vol. 111, no. 37, pp. 11047–11056, 2007.

[20] D. S. Bohle, P. Debrunner, P. A. Jordan, S. K. Madsen, and C. E. Schulz, "Aggregated heme detoxification byproducts in malarial trophozoites: β-hematin and malaria pigment have a single S= 5/2 iron environment in the bulk phase as determined by EPR and magnetic Mössbauer spectroscopy," *Journal of the American Chemical Society*, vol. 120, no. 32, pp. 8255–8256, 1998.

[21] M. A. Ambele, B. T. Sewell, F. R. Cummings, P. J. Smith, and T. J. Egan, "Synthetic hemozoin (β-hematin) crystals nucleate at the surface of neutral lipid droplets that control their sizes," *Crystal growth & design*, vol. 13, no. 10, pp. 4442–4452, 2013.

[22] L. Pauling and C. D. Coryell, "The magnetic properties and structure of hemoglobin, oxyhemoglobin and carbonmonoxyhemoglobin," *Proceedings of the National Academy of Sciences*, vol. 22, no. 4, pp. 210–216, 1936.

[23] I. Fescenko *et al.*, "Diamond magnetic microscopy of malarial hemozoin nanocrystals," *Physical review applied*, vol. 11, no. 3, p. 034029, 2019.

[24] A. Candiani, A. Argyros, S. G. Leon-Saval, R. Lwin, S. Selleri, and S. Pissadakis, "A loss-based, magnetic field sensor implemented in a ferrofluid infiltrated microstructured polymer optical fiber," *Applied Physics Letters*, vol. 104, no. 11, p. 111106, 2014.

[25] S. Azad, S. K. Mishra, G. Rezaei, R. Izquierdo, and B. Ung, "Rapid and sensitive magnetic field sensor based on photonic crystal fiber with magnetic fluid infiltrated nanoholes," *Scientific Reports*, vol. 12, no. 1, p. 9672, 2022.

[26] K. Chen, C. Yuen, Y. Aniweh, P. Preiser, and Q. Liu, "Towards ultrasensitive malaria diagnosis using surface enhanced Raman spectroscopy," *Scientific reports*, vol. 6, no. 1, pp. 1–9, 2016.

[27] C. Tempera *et al.*, "Characterization and optimization of the haemozoin-like crystal (HLC) assay to determine Hz inhibiting effects of anti-malarial compounds," *Malaria journal*, vol. 14, no. 1, pp. 1–12, 2015.

[28] T. J. Egan, D. C. Ross, and P. A. Adams, "Quinoline anti-malarial drugs inhibit spontaneous formation of β-haematin (malaria pigment)," *FEBS letters*, vol. 352, no. 1, pp. 54–57, 1994.

[29] D. S. Bohle, R. E. Dinnebier, S. K. Madsen, and P. W. Stephens, "Characterization of the products of the heme detoxification pathway in malarial late trophozoites by X-ray diffraction," *Journal of Biological Chemistry*, vol. 272, no. 2, pp. 713–716, 1997.

[30] L. M. Coronado, C. T. Nadovich, and C. Spadafora, "Malarial hemozoin: from target to tool," *Biochimica et Biophysica Acta (BBA)-General Subjects*, vol. 1840, no. 6, pp. 2032–2041, 2014.

[31] S. Nemoto, "Measurement of the refractive index of liquid using laser beam displacement," *Applied optics*, vol. 31, no. 31, pp. 6690–6694, 1992.

[32] D. Sengupta and B. Ung, "Simple optical setup for the undergraduate experimental measurement of the refractive indices and attenuation coefficient of liquid samples and characterization of laser beam profile," in *Education and Training in Optics and Photonics*, Optica Publishing Group, 2019, p. 11143_112.

[33] G. Rikken and B. A. Van Tiggelen, "Direction of optical energy flow in a transverse magnetic field," *Physical review letters*, vol. 78, no. 5, p. 847, 1997.

[34] M. Y. Darsht, I. V. Zhirgalova, B. Y. Zel'Dovich, and N. D. Kundikova, "Observation of a" magnetic" rotation of the speckle of light passed through an optical fiber," *JETP Letters*, vol. 59, no. 11, pp. 763–765, 1994.

[35] A. Butykai *et al.*, "Malaria pigment crystals as magnetic micro-rotors: key for high-sensitivity diagnosis," *Scientific reports*, vol. 3, no. 1, pp. 1–10, 2013.

[36] N. Inaba, H. Miyajima, H. Takahashi, S. Taketomi, and S. Chikazumi, "Magneto-optical absorption in infrared region for magnetic fluid thin film," *IEEE Transactions on Magnetics*, vol. 25, no. 5, pp. 3866–3868, 1989.

[37] J. Pfitzner, "Poiseuille and his law," *Anaesthesia*, vol. 31, no. 2, pp. 273–275, 1976.